

Threshold and Saturation of the Parametric Decay Instability*

R. Stenzel and A. Y. Wong

University of California, Los Angeles, California 90024

(Received 12 November 1971)

Observation of the time development of parametric instability reveals new oscillatory saturation states, whose frequency is proportional to the pump intensity. The self-consistent pump field simultaneously exhibits similar but 180° out-of-phase oscillations. Application of a small auxiliary driver wave ($E_d \sim 0.1E_0$) at the electron sideband lowers the threshold and dramatically enhances the intensity of excited ion wave. Growth rate and functional dependence of threshold on ion damping are verified.

Although the theory of parametric coupling between longitudinal electron plasma waves and ion-acoustic waves has been treated by various authors,¹⁻⁴ only very recently⁵⁻⁸ were experiments reported on the decay instability. However, neither a detailed study of the saturation mechanism nor attempts to vary the threshold have been discussed. In this Letter we describe the results of such studies on the parametric three-wave interaction in a large, uniform, Maxwellian, collisionless, magnetic-field-free plasma in which the ion and electron modes are well defined. With $T_e/T_i \gg 1$, the nonoscillatory two-stream instability is excluded since its threshold is an order of magnitude above that of the decay instability.

The experiment is performed in a double-plasma (DP) source⁹ of 40 cm diam and 50 cm length operating with argon at 0.5 mTorr. Typical plasma parameters as measured with Langmuir probes are an electron temperature $k_B T_e \approx 2$ eV, electron density $n_e \approx 10^9$ cm⁻³, ion temperature $k_B T_i \approx 0.2$ eV, and ion fluctuation level $\delta n_i/n_i \lesssim 0.1\%$. No electron or ion beam is present in the plasma. The pump rf field with frequency $f_0 = 400$ MHz $\gtrsim f_{pe}$ is provided by a parallel-plate capacitor (5-cm-diam grids, 3-cm spacing) immersed into the center of the plasma. The electrodes are coupled capacitively to the rf power amplifier in order to avoid drawing dc currents from the plasma.¹⁰ Ion waves are detected with movable Langmuir probes, electron waves with a high-impedance rf probe. Spatial correlation yields the \vec{k} spectrum. The rf pump can be pulsed with rise time of $t_r = 2$ μ sec.

Both the high-frequency (near ω_{pe}) and low-frequency ($0 < \omega < \omega_{pi}$) spectra of probe signals have been observed. For low pump field strengths the high-frequency spectrum shows a single line at $\omega = \omega_0$, while the low-frequency spectrum consists of a low level of background noise extending up to ω_{pi} . As the pump field strength is increased,

we observe at a certain threshold a second high-frequency line $\omega_2 < \omega_0$ and simultaneously a low-frequency oscillation ω_1 . The excited oscillation frequencies match with the pump, i.e., $\omega_1 + \omega_2 = \omega_0$. As the pump power is increased beyond threshold, other small sidebands appear at $\omega_0 - 2\omega_1$, $\omega_0 + \omega_1$, indicating higher-order wave coupling. Finally electron- and ion-wave spectra broaden, approaching a continuous turbulent spectrum.⁵ At present power levels no ionization effects were visible on Langmuir-probe traces.

By using two-probe spatial correlation measurements, electron and ion oscillations were identified as propagating electrostatic waves. A Langmuir probe movable in three coordinates shows that the ion propagation vector \vec{k}_i near the grids is parallel to \vec{E}_0 . At some distance from the grid, ion waves are observable over a cross section larger than the grid area indicating some spread in \vec{k}_i . The observed wave number at minimum threshold, $k_i = 6.3$ cm⁻¹, compares well with the predicted value from linear-mode coupling theory,^{1,3} $k/k_D \approx 0.2$ or $k = 5.3$ cm⁻¹. Measured ion-wave damping using the DP feature⁹ gives $\gamma_1/\omega_1 = (v_g/v_{ph})k_i/k_r \approx 10^{-2}$. Ion frequency and wave number yield a sound velocity in agreement with Langmuir-probe temperature measurements, indicating negligible frequency shift by collision frequencies

Electron plasma waves were measured with a high-impedance rf probe consisting of two parallel grids (5×5 mm², 3-mm spacing) coupled via a resonant circuit ($Z_{res} \approx 100$ k Ω) to a 50- Ω transmission line. The dispersion relation for electron plasma waves in an unbounded uniform plasma has first been verified in the range $0.15 < k/k_D < 0.35$, where collisional and Landau damping are small. Under conditions typical for the parametrically excited electron plasma wave, a damping rate $\gamma_2/\omega_2 = (v_g/v_{ph})k_i/k_r \approx 1.75 \times 10^{-3}$ is found from spatial damping measurements. The wave number of the excited plasma wave,

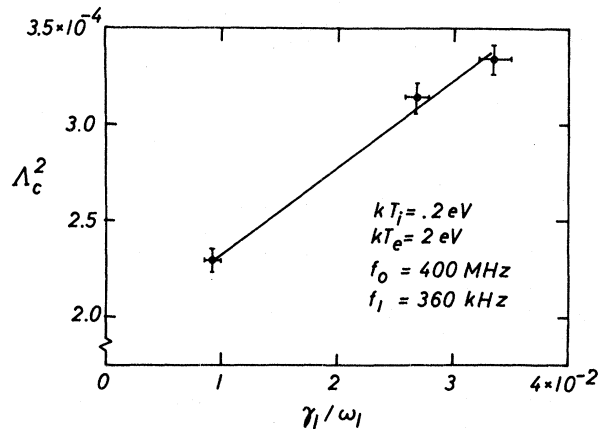


FIG. 1. Threshold pump intensity Λ_c^2 versus ion-wave damping which has been increased by adding up to 13% helium to an argon discharge.

$k_2 \approx 8 \text{ cm}^{-1}$, has been measured after frequency conversion of ω_2 with ω_0 .¹¹ The rf pump signal excites a longitudinal plasma wave with wave number k_0 . Simultaneous measurements of k_1 , k_2 , and k_0 show that wave-number matching was approximately satisfied, $\vec{k}_1 + \vec{k}_2 \approx \vec{k}_0$.

After calibrating the high-impedance probe in a known, uniform rf field in vacuum,¹² the peak electric field inside the grid capacitor at instability threshold has been determined as $E_0 \approx 2.5 \text{ V/cm}$ or $\Lambda_c^2 = E_0^2 / 16\pi m k_B T_e \approx 2.2 \times 10^{-4}$. The theoretically predicted value,³ based on our measured damping rates, yields

$$\Lambda_c^2 = 4 \frac{\gamma_1}{\omega_1} \frac{\gamma_2}{\omega_2} \left(1 + \frac{\gamma_2^2}{4\omega_1^2} \right) = 1.3 \times 10^{-4}. \quad (1)$$

The difference lies within the combined measurement uncertainties for the electric field and damping rates.

The dependence of the threshold intensity on ion-wave damping has been investigated (Fig. 1). Adding a small percentage of light ion impurities (He) increases γ_1/ω_1 which is directly measured by ion-acoustic wave propagation in the DP machine. An increase in the threshold intensity proportional to γ_1/ω_1 is observed. The slope of Λ_c^2 vs γ_1/ω_1 yields an independent measure for γ_2/ω_2 (1.05×10^{-3}) which is consistent with the direct measurement.

The evolution from the linear growth regime to the nonlinear saturation state has been studied by gating the pump signal (5-kHz square wave). Although the applied rf signal is constant during the turn-on period, the self-consistent pump field exhibits fluctuations which are correlated with

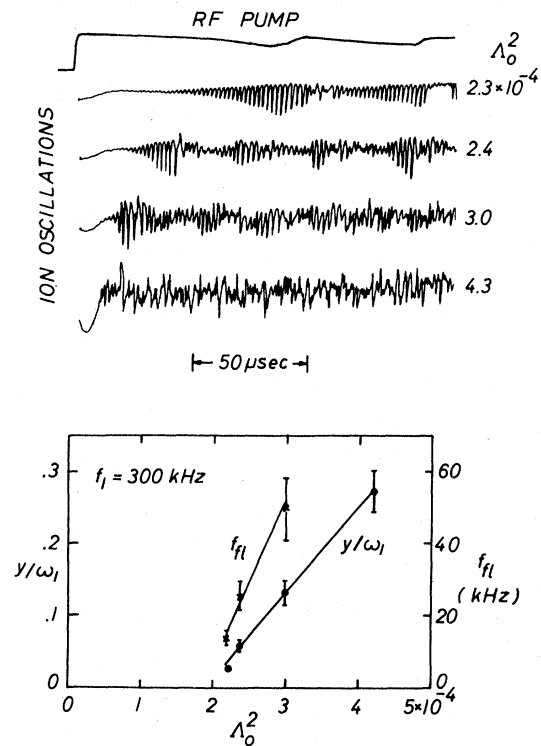


FIG. 2. Top: Self-consistent pump field and ion oscillation amplitude after turning on the pump. Bottom: Normalized growth rate y/ω_1 and fluctuation frequency f_{fl} versus pump intensity.

the excited ion and electron oscillations. As shown in Fig. 2 (top two traces) the pump amplitude decreases as the ion oscillations build up indicating energy exchange between the pump and the sidebands.^{1, 13, 14}

Close to threshold, electron and ion oscillations show an exponential growth rate y/ω_1 proportional to the pump intensity in agreement with the expected behavior¹

$$y/\omega_1 = \frac{1}{4} (\omega_2/\gamma_2) \Lambda_0^2 - \gamma_1/\omega_1. \quad (2)$$

The observed growth rate near threshold is in good agreement with the above expression. The slope of the growth rate y/ω_1 vs Λ_0^2 yields another measure for γ_2/ω_2 (4×10^{-3}) which supports the direct measurement ($\gamma_2/\omega_2 = 1.75 \times 10^{-3}$).

The oscillations saturate at an amplitude independent of the pump intensity indicating an amplitude-limiting saturation process. In the saturation regime the amplitude fluctuates¹⁴ at a low frequency $f_{fl} < f_1$ which increases linearly with pump intensity (Fig. 2).

Under steady-state conditions the intensity of the ion wave, $I_1 = (1/2\pi) \int E_1^2(k_1, \omega_1) d\omega$, is much

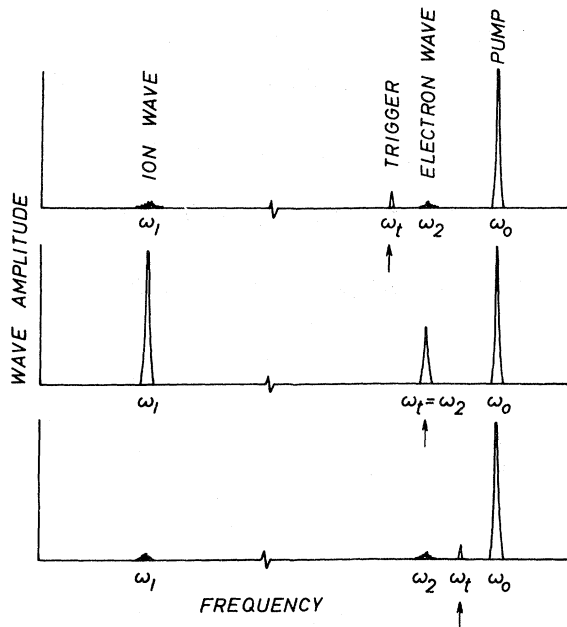


FIG. 3. The decay instability $\omega_0 \rightarrow \omega_1 + \omega_2$ is induced when a small trigger signal is frequency matched with the weakly damped electron plasma wave.

smaller than that of the electron wave, I_2 , as required by the Manley-Rowe relation. Near threshold we find $I_1/I_2 \approx E_1^2/E_2^2 = 2.5 \times 10^{-3}$, where $E_1 = k_1(k_B T_e/e)\delta n_1/n = 1.3 \times 10^{-2}$ V/cm and $E_2 \approx 0.1E_0 = 0.25$ V/cm. Theoretical calculations of the nonlinear saturation intensities by DuBois and Goldman¹⁵ predict

$$I_1/I_2 = \frac{1}{16} \Lambda^2 (k/k_D)^2 (\omega_1/\gamma_1)^2 \approx 5.5 \times 10^{-3} \quad (3)$$

which is in reasonable agreement with our observations.

The threshold of the parametric instability is drastically lowered when an additional small-amplitude electron plasma wave ($\Lambda_t^2/\Lambda_0^2 \approx 10^{-2}$) is excited and its frequency adjusted to the instability frequency, $\omega_t = \omega_2 = \omega_0 - \omega_1$, as schematically shown in Fig. 3. Near threshold the ion-wave intensity is 10 to 20 dB higher than in the case of a single pump; the saturation level is also increased (Fig. 4). We believe the driver wave initiates the parametric process much more effectively than background thermal fluctuations and enhances the energy transfer from the pump into a single pair of electron and ion waves instead of a spread into many unstable modes.

When the driver wave is tuned to the weakly excited lines $\omega_t = \omega_0 + \omega_1$ (anti-Stokes line) and $\omega_t = \omega_0 - 2\omega_1$, we also find an enhanced ion-wave intensity at ω_1 . However, this driving mode re-

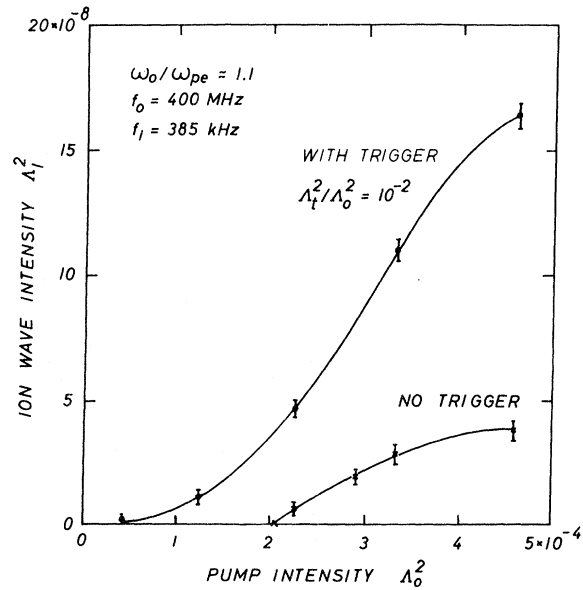


FIG. 4. Enhancement of the decay instability with a small trigger wave.

quires higher intensities ($\Lambda_t^2/\Lambda_0^2 \approx 10^{-1}$).

The authors are indebted to Dr. D. F. DuBois and Dr. M. V. Goldman for stimulating discussions, and to Mr. Zalton Lucky and Mr. D. Woolley for technical support.

*Research supported by the U. S. Air Force Office of Scientific Research under Grant No. AFOSR 71-2080.

¹D. F. DuBois and M. V. Goldman, Phys. Rev. Lett. **14**, 544 (1965), and Phys. Rev. **164**, 207 (1967), and Phys. Rev. Lett. **19**, 1105 (1967).

²P. K. Kaw and J. M. Dawson, Phys. Fluids **12**, 2586 (1969).

³K. Nishikawa, J. Phys. Soc. Jap. **24**, 916, 1152 (1968).

⁴P. K. Kaw and J. M. Dawson, Phys. Fluids **12**, 2586 (1969).

⁵R. Stenzel, University of California at Los Angeles Plasma Physics Group Report No. R-84 (unpublished); A. Y. Wong, F. F. Chen, N. Booth, D. L. Jassby, R. Stenzel, D. Baker, and C. S. Liu, in Proceedings of the Fourth Conference on Plasma Physics and Controlled Nuclear Fusion Research, Madison, Wisconsin, June 1971 (unpublished), paper No. B-15.

⁶A. Y. Wong and R. J. Taylor, Phys. Rev. Lett. **27**, 644 (1971); the electron distribution in the ionosphere could be non-Maxwellian.

⁷H. Dreicer, D. B. Henderson, and J. C. Ingraham, Phys. Rev. Lett. **26**, 1616 (1971).

⁸R. N. Franklin, S. M. Hamberger, G. Lampis, and G. J. Smith, Phys. Rev. Lett. **27**, 1119 (1971). This experiment was performed for plasma conditions quite different from ours: $T_e/T_i = 1$, non-Maxwellian ion dis-

tribution, one-dimensional, axially magnetized plasma column.

⁹H. Ikezi and R. J. Taylor, Phys. Rev. Lett. 22, 923 (1969), and J. Appl. Phys. 41, 738 (1970); R. J. Taylor, D. R. Baker, and H. Ikezi, Phys. Rev. Lett. 24, 206 (1970).

¹⁰K. Takayama and H. Ikegami, Phys. Rev. Lett. 5, 238 (1960).

¹¹It is worth noting that the sign of \vec{k}_2 is reversed in the conversion with $\omega_0 > \omega_2$.

¹²In using the rf probe in a plasma, the grids are surrounded by sheaths. In an equivalent probe circuit the

sheaths can be approximated by capacitors $C_{eq} \approx \epsilon_0 A / 3\lambda_D$ in series with a voltage source. Since the load resistance $Z_{res} \approx 100 \text{ k}\Omega$ is much larger than the sheath reactance $2/\omega C_{eq} \approx 3.5 \text{ k}\Omega$, the error in the measured electric field is small.

¹³A. Y. Wong, M. V. Goldman, F. Hai, and R. Rowberg, Phys. Rev. Lett. 21, 518 (1968).

¹⁴R. Z. Sagdeev and A. A. Galeev, *Nonlinear Plasma Theory*, edited by T. M. O'Neil and D. L. Book (Benjamin, New York, 1969).

¹⁵D. F. DuBois and M. V. Goldman, Phys. Rev. Lett. 28, 218 (1972).

Attenuation and Velocity of Sound in Superfluid Helium*

Humphrey J. Maris

Physics Department, Brown University, Providence, Rhode Island 02912

(Received 22 November 1971)

The attenuation and velocity of sound in liquid He⁴ have been calculated using the Landau-Khalatnikov kinetic equations and the phonon Boltzmann equation. A detailed comparison between theory and experiment is made at 0.35°K and good agreement is obtained over a wide range of frequencies.

In this Letter we consider the attenuation and velocity of sound in liquid He⁴. We will concentrate on the temperature range below 0.6°K where rotons may be neglected. Although there has been much theoretical effort, no satisfactory explanation of the attenuation and velocity at these temperatures has yet been given.¹ The theories have generally assumed that the energy-momentum relation for low-energy phonons has the form

$$\epsilon(p) = c_0 p (1 - \gamma p^2 + \dots), \quad (1)$$

where c_0 and γ are positive quantities. In a previous Letter² it was proposed that γ is negative, thus making the dispersion anomalous in that the group velocity v_p increases with increasing p in the small- p regime. This idea radically changes the traditional approach³ to phonon-phonon interactions in He⁴ because three-phonon collisions that conserve energy and momentum may now occur. The proposal that $\gamma < 0$ has since received support from specific-heat measurements.⁴

In this Letter we report the results of detailed calculations of the attenuation and velocity of sound assuming that $\gamma < 0$. The agreement between these calculations and the experimental results of Abraham *et al.*¹ and Waters, Watmough, and Wilks⁵ is remarkably good and constitutes strong evidence that γ is indeed negative. We also propose additional experiments to test the theory.

The starting point of our calculation is the kinetic equations of Landau and Khalatnikov.³ These are

$$\partial \rho / \partial t + \text{div}(\rho \vec{v}_s + \int \vec{p} n_p d\tau_p) = 0, \quad (2)$$

$$\partial \vec{v}_s / \partial t + \nabla[\mu_0 + \frac{1}{2} v_s^2 + \int (\partial \epsilon / \partial p) n_p d\tau_p] = 0, \quad (3)$$

where ρ is the density, \vec{v}_s the superfluid velocity, μ_0 the chemical potential at absolute zero, and n_p the number of phonons of momentum \vec{p} . The integrals are over all of momentum space. We look for a solution of these equations in the form of a wave propagating in the z direction with wave vector \vec{K} and frequency Ω . Consequently, we define $\Delta \rho$ and Δn_p by

$$\rho = \rho_0 + \Delta \rho \exp[i(2\pi Kz - \Omega t)], \quad (4)$$

$$n_p = \tilde{n}_p + \Delta n_p \exp[i(2\pi Kz - \Omega t)], \quad (5)$$

where

$$\tilde{n}_p = \{ \exp[\beta(\epsilon + \vec{p} \cdot \vec{v}_s)] - 1 \}^{-1}, \quad (6)$$

ρ_0 is the density at $T = 0^\circ\text{K}$, and $\beta = (k_B T)^{-1}$. Note that \tilde{n}_p depends upon z and t because \vec{v}_s is space and time dependent, and also because ϵ depends on p . The attenuation α and the velocity correction Δc relative to the velocity c_0 at absolute zero